Itsarawisut, J., Laosuwan, T., Uttaruk, Y., Rotjanakusol, T., Laosuwan, N., Peebkhunthod, T., Singharaj, M. (2026). Estimation of forest aboveground biomass and carbon stock using sentinel-2 vegetation indices and exponential regression in a tropical dry dipterocarp forest. Agriculture and Forestry, 72 (2): 103-122. https://doi:10.17707/AgricultForest.72.2.08

DOI: 10.17707/AgricultForest.72.2.08

Jumpol ITSARAWISUT[1,2], Teerawong LAOSUWAN*[1,4], Yannawut UTTARUK[3,4], Tanutdech ROTJANAKUSOL[1,4], Natcha LAOSUWAN[1,4], Thanakrizt PEEBKHUNTHOD[5], Maharaja SINGHARAJ[6]

ESTIMATION OF FOREST ABOVEGROUND BIOMASS AND CARBON STOCK USING SENTINEL-2 VEGETATION INDICES AND EXPONENTIAL REGRESSION IN A TROPICAL DRY DIPTEROCARP FOREST

SUMMARY

This study presents a quantitative approach for estimating aboveground biomass (AGB) and carbon stock in a tropical dry forest ecosystem by integrating Sentinel-2 multispectral imagery with field inventory data. Six field plots (40×40 m) were established in the Mahasarakham University forest area, Thailand, where 1,127 trees representing 61 species were measured for diameter and height. The total AGB was estimated at 71.92 t, corresponding to an average carbon density of 35.21 tC ha^{-1}. Three vegetation indices derived from Sentinel-2 imagery (NDVI, SAVI, and MSAVI2) were converted to fractional vegetation cover using exponential relationships. Among the tested models, MSAVI2 showed the strongest correlation with field-based carbon estimates (R^2=0.839), producing a total carbon stock of 1,752.87 tC, closely matching the observed value (1,807.72 tC) with a difference of –3.0%. SAVI demonstrated the highest predictive accuracy with the lowest RMSE (0.901 t ha^{-1}; RMSE%=1.34%). The results

[1]Jumpol Itsarawisut, Teerawong Laosuwan (corresponding author: teerawong@msu.ac.th), Tanutdech Rotjanakusol, Natcha Laosuwan, Department of Physics, Faculty of Science, Mahasarakham University, Maha Sarakham, 44150, THAILAND;

[2]Jumpol Itsarawisut, Space Technology and Geoinformatics Research Unit, Faculty of Science, Mahasarakham University, Maha Sarakham, 44150, THAILAND;

[3]Yannawut Uttaruk, Department of Biology, Faculty of Science, Mahasarakham University, Maha Sarakham, 44150, THAILAND;

[4]Teerawong Laosuwan, Yannawut Uttaruk, Tanutdech Rotjanakusol, Natcha Laosuwan, Greenhouse Gas Research Center and Operations, Faculty of Science, Mahasarakham University, Maha Sarakham, THAILAND.

[5]Thanakrizt Peebkhunthod, Mahasarakham University Demonstration School, Mahasarakham University, Maha SaraKham, 44150, Thailand.

[6]Maharaja Singharaj, Geographic Information Science, School of Information and Communication Technology, University of Phayao, 56000, Thailand.

Notes: The authors declare that they have no conflicts of interest. Authorship Form signed online.

Recieved:22/03/2026 *Accepted:23/04/2026*

confirm that Sentinel-2–based exponential models provide reliable and cost-effective tools for large-scale forest biomass and carbon assessment. This approach offers practical potential for forest management, carbon monitoring, and sustainable land-use planning under regional and international carbon-credit frameworks.

Keywords: aboveground biomass; carbon stock; sentinel-2; vegetation indices; tropical dry dipterocarp forest; remote sensing

INTRODUCTION

Climate change is among the most serious environmental issues of the 21st century—largely brought about by enhanced concentration of greenhouse gases (GHGs) in the atmosphere. Anthropogenic sources such as fossil fuel combustion, and land-use change and deforestation are primary sources of carbon dioxide (CO_2) emissions (IPCC, 2014). Increase in GHG concentrations retain heat of atmosphere that result in elevated temperature (global warming), climate variability and extremes (Angkahad *et al.*, 2024). It is thus important to observe the carbon sources and sinks in terrestrial ecosystems for mitigating climate change. Assessment of carbon losses is an important component of national carbon accounting, and informs climate policy and ecosystem management. The United Nations Framework Convention on Climate Change (UNFCCC) recommends that developing countries apply the Intergovernmental Panel on Climate Change (IPCC) guidelines for estimating CO_2 emissions (UNFCCC, 1992). These guidelines are particularly important for assessing emissions from land-use change and forest degradation (UNFCCC, 2010).

Developing reliable models requires detailed information on forest degradation, carbon emissions, and forest conditions after disturbance. Such information is commonly obtained through field inventories and remote sensing techniques. Forest degradation is one of the main causes of carbon stock reduction (Yu *et al.*, 2024) and is frequently associated with deforestation activities (Bullock and Woodcock, 2021). At the global scale, it contributes approximately 12–20% of total greenhouse gas emissions (Grantham Research Institute on Climate Change and the Environment, 2023). Pearson *et al.*, (2017) estimated that developing countries collectively release about 2.1 billion tonnes of CO_2 each year as a result of forest degradation. Ritchie (2021) reported that around 10 million hectares of forest are cleared annually worldwide; however, the net global forest loss between 2010 and 2020 was closer to 4.7 million hectares per year when afforestation and natural forest regrowth were taken into account. Supporting this global perspective, McNicol *et al.*, (2018) found that in Southern African woodlands, forest degradation affected nearly 17% of the wooded area and was responsible for approximately 55% of biomass loss (~0.075 PgC per year), which was considerably higher than the losses caused by deforestation alone (~0.038 PgC per year). These findings highlight that forest degradation can play an even more important role than deforestation in driving carbon loss in many forest ecosystems.

The impacts of forest degradation are not limited to carbon accounting. Changes in regional biomass can also affect ecosystem structure and functioning. This issue is recognized within global REDD+ frameworks, which aim to address both deforestation and forest degradation under climate mitigation strategies (Samek *et al.,* 2014). Biomass is commonly divided into five major carbon pools: aboveground biomass (AGB) (Uttaruk and Laosuwan, 2020a; Uttaruk and Laosuwan, 2020b), belowground biomass, soil organic matter (SOM), deadwood, and litter (Kulmann *et al*., 2022). Among these components, AGB is particularly important because it serves as a key indicator of CO_2 emissions from deforestation (Plybour *et al.,* 2025) and provides insight into broader climate change dynamics. Carbon loss can reduce ecosystem stability and functioning, highlighting the need for systematic assessment (Laosuwan *et al*., 2023; Uttaruk *et al.,* 2024). Previous studies on land-use carbon emissions have mainly focused on carbon accounting (Andreoni and Galmarini, 2016; Carpio *et al*., 2021; Laosuwan *et al.,* 2025a). In such cases, accurate estimation of AGB loss is essential for quantifying CO_2 emissions (Awichin *et al*., 2025; Laosuwan *et al.,* 2025b). Traditionally, species-specific allometric equations have been widely used to estimate AGB (Aneseyee *et al.,* 2021; Uttaruk *et al*., 2026). These equations are based on measurable tree attributes such as diameter at breast height (DBH), tree height, and wood density, which describe scaling relationships between tree structure and biomass accumulation processes (Duangsathaporn *et al.,* 2023; Sun *et al*., 2024).

The development of satellite-based monitoring systems has significantly improved forest biomass estimation by enabling large-scale assessments (Mkuzi *et al*., 2025). Currently, allometric equations derived from field measurements are often combined with remote sensing data to produce more comprehensive estimates of aboveground biomass (AGB) and carbon stock in forest ecosystems (Uttaruk and Laosuwan, 2018; Laosuwan *et al*., 2024). Remote sensing approaches have become widely used because they offer several advantages, including repeatable data acquisition and strong relationships between spectral reflectance and vegetation characteristics (Askar *et al.,* 2018; Angkahad *et al.*, 2025). However, spatial resolution remains a critical factor, as it influences image texture analysis and the ability to distinguish different land-cover types, particularly in forests with complex stand structures (Kulawardhana *et al*., 2014). Houghton *et al*., (2009) highlighted that satellite observations allow biomass and carbon flux patterns to be quantified and mapped consistently from regional to global scales.

Increasingly, field-based quadrat data are being integrated with remotely sensed imagery in forest studies (Vicharnakorn *et al.,* 2014), allowing predictive models to be developed for monitoring aboveground biomass (AGB) and estimating carbon stocks (Somprasong, 2024). Modern satellite platforms provide data with various spatial, temporal, and spectral resolutions (Samphutthanont *et al.,* 2024). In subtropical forests, studies have shown that imagery with coarse spatial resolution and broad spectral bands may be insufficient to capture high species diversity and complex stand structures (Mutanga *et al.,* 2012; Vahtmäe *et al.,* 2021). In contrast, datasets with finer spatial resolution and narrower spectral bands generally provide more reliable and accurate AGB estimates. Among available sensors, Sentinel-2 multispectral imagery, with a spatial resolution of 10 m, has been recognized as valuable for regional to global biomass assessments (Sousa Júnior *et al.,* 2023). When combined with ground-based plot inventories, its spectral bands, vegetation indices (VIs), and derived biophysical parameters can significantly improve model robustness and prediction accuracy for AGB estimation (Israel *et al.,* 2025). Sentinel-2 data are freely available through the European Space Agency (ESA), making this approach accessible for operational biomass mapping (Faria *et al.*, 2024; Liu *et al.*, 2024). Accurate quantification of biomass loss is essential not only for evaluating the impacts of deforestation on ecosystem function and climate change, but also for supporting international forest monitoring frameworks and national greenhouse gas inventories, as well as for meeting the UNFCCC net-zero emission targets.

Although previous studies have used Sentinel-2 data and vegetation indices with regression models to estimate biomass, most of them focus on tropical humid forests or plantation areas. Tropical dry dipterocarp forests are still less studied. In addition, many studies apply complex machine learning methods, which may not be suitable for areas with limited data or resources. This study focuses on a dry dipterocarp forest and develops a simple exponential model. The model uses NDVI, SAVI, and MSAVI2 to estimate aboveground biomass and carbon stock. The method is easy to apply and requires low cost. It can support carbon monitoring and MRV systems. It is also suitable for both national and international carbon credit projects. Therefore, this study aims to develop and validate an exponential regression model using Sentinel-2 vegetation indices and field data. The results can improve biomass estimation and support practical applications in forest management and carbon assessment.

MATERIAL AND METHODS

Study Area

The research was conducted in the forested area of Mahasarakham University Farm, located in Na Si Nuan Subdistrict, Kantharawichai District, Maha Sarakham Province, Thailand (16.2622° N, 103.2683° E) (Figure 1). The study site covers approximately 62.9 ha at an elevation of about 153 m above mean sea level. The terrain is characterized by a gently undulating plateau without mountainous features. Maha Sarakham Province has a tropical monsoon climate with three distinct seasons: winter (mid-October to mid-February), summer (mid-February to mid-May), and the rainy season (mid-May to mid-October). Based on long-term climatic data (1981–2010), the mean annual temperature is 27.4 ℃, ranging from 22.4 ℃ to 33.7 ℃, with April being the hottest month. The average annual rainfall ranges between 1,000 and 1,200 mm, providing favorable conditions for maintaining natural forest cover in the area.

The vegetation of the study site is predominantly dry dipterocarp forest mixed with deciduous species. Dominant tree species include Shorea siamensis, *Dipterocarpus obtusifolius*, *Xylia xylocarpa*, *Pterocarpus macrocarpus*, and *Terminalia alata*, forming a moderately dense canopy layer approximately 10–15 m in height. The understory consists of shrubs and ground vegetation such as Imperata cylindrica and leguminous herbs, which contribute to soil fertility through nitrogen fixation. The soils are mainly sandy loam to sandy clay loam with moderate fertility and good drainage capacity. The area has been designated as a long-term research and conservation zone under the "Mahasarakham University Green Campus and Carbon Management Program," serving as a representative ecosystem for monitoring aboveground biomass, carbon dynamics, and biodiversity in northeastern Thailand.

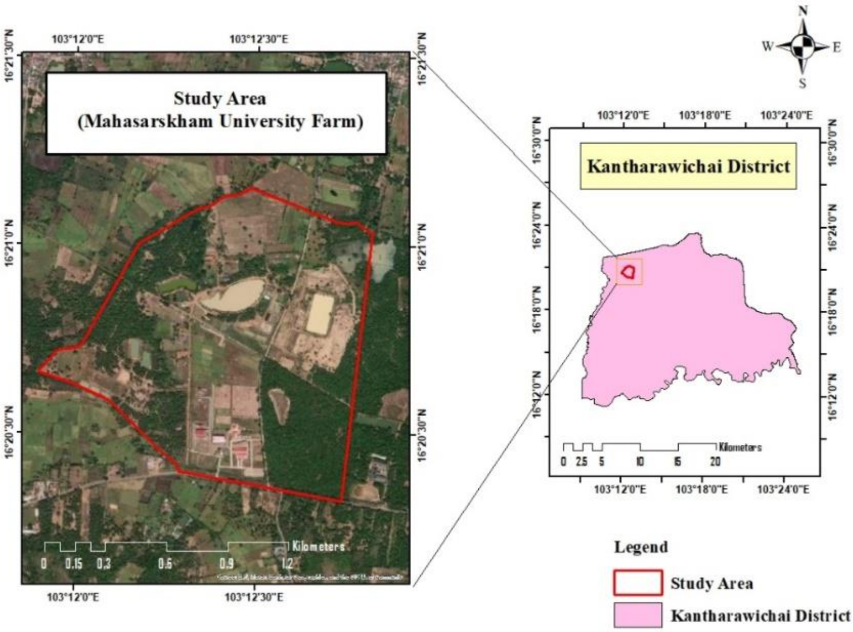

Figure 1. Location of the study area at Mahasarakham University Farm, Maha Sarakham Province, Thailand.

Field data collection

Field data were collected to record tree species composition and structural characteristics within the study area. Sampling was conducted in six square plots, each measuring 40×40 m. The sampling design in this study follows the guideline for forest carbon assessment, which suggests that approximately 1% of the project area should be used for plot-based sampling under random sampling conditions (TGO, 2017). The plots were distributed across the study area to represent different canopy conditions. This sampling design meets the minimum requirement for small-scale forest projects and provides adequate representation of field conditions. However, the authors acknowledge that the sample size is still limited in terms of spatial coverage. Although the sampling design is sufficient for model development and preliminary assessment, future studies should include more plots and wider spatial distribution to improve statistical robustness and model generalization.

In each plot, all trees with a diameter at breast height (DBH) greater than 4.5 cm were measured. DBH was recorded using a diameter tape, and tree height (*H*) was measured with a laser rangefinder. These parameters are commonly used indicators of tree size and stand structure. The field measurements were converted into aboveground biomass (AGB) using allometric equations (Equation 1) developed by Ogawa *et al.*, (1965). The estimated AGB values were then converted into carbon stock using a biomass-to-carbon conversion factor (Equation 2) following the Intergovernmental Panel on Climate Change guidelines (IPCC, 2006). This approach integrates field measurements with biomass estimation models to quantify carbon storage at the local scale.

$$\begin{aligned} W_S &= 0.0396(D^2H)^{0.933} \\ W_B &= 0.00349(D^2H)^{1.030} \\ W_L &= \left(\frac{28}{W_S + W_B} + 0.025\right)^{-1} \\ W_T &= W_S + W_B + W_L \end{aligned} \tag{1}$$

In this study, *D* represents the diameter at breast height (cm), while H corresponds to the total tree height (m). The aboveground biomass components are defined as follows: *WS* for stem biomass (t ha^{-1}), *WB* for branch biomass (t ha^{-1}), *WL* for leaf biomass (t ha^{-1}), and *WT* for the sum of all aboveground biomass (t ha^{-1}).

$$C_j = W_{tc} \times FC \tag{2}$$

In this context, C_j denotes the carbon retention potential of a single tree (kg), W_tc expresses its aboveground biomass (kg), and *FC* is the biomass-to-carbon conversion ratio, taken as a constant value of 0.47 (IPCC, 2006).

Satellite data analysis

In this study, Sentinel-2 satellite imagery was used to assess vegetation characteristics in the study area. Three vegetation indices were selected: NDVI (Tucker *et al.*, 1979), SAVI (Huete, 1988), and MSAVI2 (Qi, 1994), as shown in Equations 3–5. These indices are widely used to represent vegetation condition and density. The index values were then converted into Fractional Green Vegetation Cover (FC) using Equation 6. This step allows spectral data to be expressed as vegetation cover. NDVI, SAVI, and MSAVI2 were selected due to their simplicity and effectiveness. SAVI and MSAVI2 are designed to reduce soil background effects. This is important in dry dipterocarp forests where vegetation cover is relatively sparse. However, in this study, other indices such as the Enhanced Vegetation Index (EVI) were not included. EVI is more sensitive in dense vegetation but requires additional parameters and more complex processing. This limitation is acknowledged, and future studies should consider including additional indices.

$$NDVI = \frac{NIR - RED}{NIR + RED} \tag{3}$$

In this formulation, *NIR* represents the reflectance of the near-infrared band, while *Red* corresponds to the reflectance of the red band. The resulting index is a dimensionless metric with values ranging from –1.0 to 1.0, where higher values signify greater vegetation density.

$$SAVI = \frac{(NIR - RED) \times (1 + L)}{(NIR + RED + L)} \tag{4}$$

NIR denotes the reflectance in the near-infrared band, Red represents the reflectance in the red band, and *L* is the soil brightness correction factor that reduces the influence of soil background on the vegetation signal. The value of *L* generally ranges from 0 for areas with very dense vegetation to 1 for bare soil, with 0.5 commonly applied in regions with moderate vegetation cover.

$$MSAVI2 = (1/2) * (2(NIR + 1) - sqrt((2 * NIR + 1)^2 - 8\left(NIR - Red\right))) \tag{5}$$

In this equation, *NIR* refers to the near-infrared spectral band, while Red corresponds to the red band. The *MSAVI2* index was developed to minimize the impact of exposed soil on vegetation measurements, making it particularly suitable for regions with low or patchy vegetation cover.

$$FC = \frac{VI_i - VI_s}{VI_v - VI_s} \tag{6}$$

In this context, VI_i refers to the vegetation index value of pixel i, while VIs represents the index value associated with bare soil or non-vegetated surfaces, and *VIv* corresponds to the value observed in fully vegetated pixels. The selection of appropriate *VIs* and *VIv* reference values is generally based on information from prior research or established soil and vegetation databases.

Development of the Exponential Regression Model

The relationship between Fractional Green Vegetation Cover (FC) and aboveground biomass (AGB) density was analyzed using an exponential regression model. This approach is widely used for biomass estimation from Sentinel-2 satellite data. The model is presented in Equation 7. The model was used to describe the relationship between vegetation indices (NDVI, SAVI, and MSAVI2) and field-measured AGB. Model parameters were estimated using regression analysis in Microsoft Excel. Due to the limited sample size, a separate validation dataset was not used. Model performance was evaluated using the coefficient of determination (R^2) and root mean square error (RMSE). These indicators provide a basic assessment of model accuracy and reliability.

$$AGB = a \times b^{e \times FC} \tag{7}$$

In this equation, a denotes the intercept of the regression curve, while b represents the regression coefficient, which governs the rate at which biomass increases as FC values rise. The results indicated that AGB exhibits an exponential growth pattern with increasing FC, thereby confirming a strong and consistent positive relationship between vegetation cover and biomass accumulation within the study area.

Model Validation through Root Mean Square Error (RMSE)

The predictive accuracy of the developed model for estimating aboveground biomass (AGB) density was evaluated by comparing field observations with model-generated estimates. Performance assessment was conducted using the Root Mean Square Error (RMSE), as shown in Equation 8. This statistical metric is derived by calculating the differences between observed and predicted values, squaring each difference, computing their mean, and then taking the square root of that mean. The RMSE value obtained indicates the extent of variation between predicted and actual measurements. Lower RMSE values correspond to higher model precision and reduced prediction error. In the present study, where Sentinel-2–based vegetation indices were applied for AGB estimation, RMSE provided an essential benchmark for validating model reliability. Beyond validation, RMSE also functions as a diagnostic measure to detect possible sources of error, thereby supporting further refinement of the model and enhancing the robustness of biomass estimation across diverse forest environments.

$$RMSE = \sqrt{\Sigma \left(Pi - Oi\right)^2 / n} \tag{8}$$

In this equation, P_i denotes the predicted biomass derived from vegetation indices, O_i represents the observed biomass measured in the field, and n is the total number of samples.

RESULTS AND DISCUSSION

This section presents the results of the study, starting with field-based measurements and the estimation of aboveground biomass (AGB) and carbon stock. These findings are followed by an analysis of vegetation indices, the development of regression models, and an evaluation of their predictive performance. The discussion then integrates these results to highlight key patterns, explain their ecological significance, and examine the potential of remote sensing approaches for large-scale biomass and carbon stock estimation.

Result of Field data collection

A total of 1,127 trees representing 61 species were recorded in the study area.

The ten most abundant species are presented in Table 1, ranked by their frequency of occurrence. *Dipterocarpus obtusifolius* was the dominant species, with 233 individuals, followed by *Xylia xylocarpa* (120 individuals) and *Rothmannia wittii* (65 individuals). The remaining species among the top ten ranged from 32 to 58 individuals, indicating a moderate level of species diversity within the forest stand.

Table 1. The ten most abundant tree species recorded in the study area

Rank	Scientific name	Number of individuals
1	Dipterocarpus obtusifolius	233
2	Xylia xylocarpa	120
3	Rothmannia wittii *(Craib) Bremek.*	65
4	*Hesperethusa crenulata* (Roxb.) Roem.	58
5	Memecylon edule Roxb.	55
6	Cratoxylum formosum (Jacq.) Benth. & Hook.f. ex Dyer (*C.* formosum *subsp.* formosum)	54
7	Sindora siamensis	50
8	Cratoxylum formosum (Jacq.) Benth. & Hook.f. ex *Dyer subsp.* pruniflorum (Kurz) Gogelein	43
9	Ellipanthus tomentosus Kurz	33
10	Catunaregam tomentosa (Blume ex DC.) Tirveng.	32

Aboveground biomass (AGB) was estimated by partitioning total biomass into stem, branch, and leaf components. The results showed that stem biomass (Ws) contributed the largest proportion, amounting to 58,034.76 kg (58.035 t). Branch biomass (Wb) accounted for 11,763.19 kg (11.763 t), while leaf biomass (Wl) represented the smallest fraction at 2,117.99 kg (2.118 t). The total AGB was therefore 71,915.93 kg (71.916 t).

The dominance of *Dipterocarpus obtusifolius* is consistent with the typical structure of dry dipterocarp forests in northeastern Thailand, where this species commonly forms the main canopy layer. The relatively high abundance of *Xylia xylocarpa* and *Sindora siamensis* also reflects the adaptation of these hardwood species to local environmental conditions. The predominance of stem biomass highlights the structural importance of tree stems in biomass accumulation and carbon storage compared with branches and leaves. Similar patterns have been reported in tropical dry forests, where stem components account for the majority of biomass due to their role in supporting tree growth and long-term carbon sequestration. Overall, species composition and biomass partitioning play important roles in determining biomass distribution and carbon dynamics within the studied ecosystem.

To enable spatial comparison among sampling units, aboveground biomass (AGB) and carbon stock were expressed on a per-hectare basis (t ha^{-1}; tC ha^{-1}). Plot-level values and summary statistics (sum, mean, and standard deviation) are presented in Table 2, while the distribution of carbon density across the six plots, together with the overall mean value, is illustrated in Figure 2. Carbon estimates were derived using the biomass-to-carbon conversion described in the methods section. Table 2 and Figure 2 together illustrate both the central tendency and variability of carbon storage, highlighting differences among plots within the study area.

Table 2. Aboveground biomass (AGB) and carbon stock per plot (tC ha^{-1})

Plot	AGB (t ha^{-1})	Carbon (tC ha^{-1})
1	78.187	36.748
2	42.834	20.132
3	48.897	22.982
4	137.529	64.639
5	87.439	41.097
6	54.587	25.656
Sum (6 plots)	449.473	211.252
Mean	74.912	35.209
SD (sample)	35.235	16.560

Table 2 shows clear variation among plots. Plot 4 recorded the highest values (AGB=137.529 t ha^{-1}; Carbon=64.639 tC ha^{-1}), which is likely associated with a greater presence of large trees and higher stand density. In contrast, Plot 2 showed the lowest values (AGB=42.834 t ha^{-1}; Carbon=20.132 tC ha^{-1}). On average across the six plots, AGB was 74.912 t ha^{-1} and carbon stock was 35.209 tC ha^{-1}, with standard deviations of 35.235 t ha^{-1} and 16.560 tC ha^{-1}, respectively, indicating substantial structural heterogeneity within the forest stand. As expected, a positive relationship between AGB and carbon storage was observed, with plots containing higher biomass also storing more carbon. Differences among plots likely reflect variation in canopy cover, stem size distribution, and species composition. Scaling the mean per-hectare values to the study area (62.88 ha) resulted in estimated totals of approximately 4,710.48 t AGB and 2,213.92 tC, highlighting the role of this forest as an important local carbon sink and providing a quantitative baseline for management and monitoring.

The bars in Figure 2 represent carbon density for each plot, while the horizontal dashed line indicates the mean value (35.209 tC ha^{-1}; biomass-to-carbon conversion following IPCC, 2006). Carbon density ranged from 20.132 to 64.639 tC ha^{-1}, with a standard deviation of 16.560 tC ha^{-1} and a coefficient of variation of approximately 47%, suggesting considerable structural variation among sampling units. A slight right-skew distribution is evident due to the relatively high value observed in Plot 4. Relative differences from the mean further illustrate variability among stands: Plot 4 showed a carbon density 84% higher than the mean, whereas Plot 2 was approximately 43% lower. Plot 1 was closest to the average value (36.748 tC ha^{-1}; +4%), representing typical site conditions.

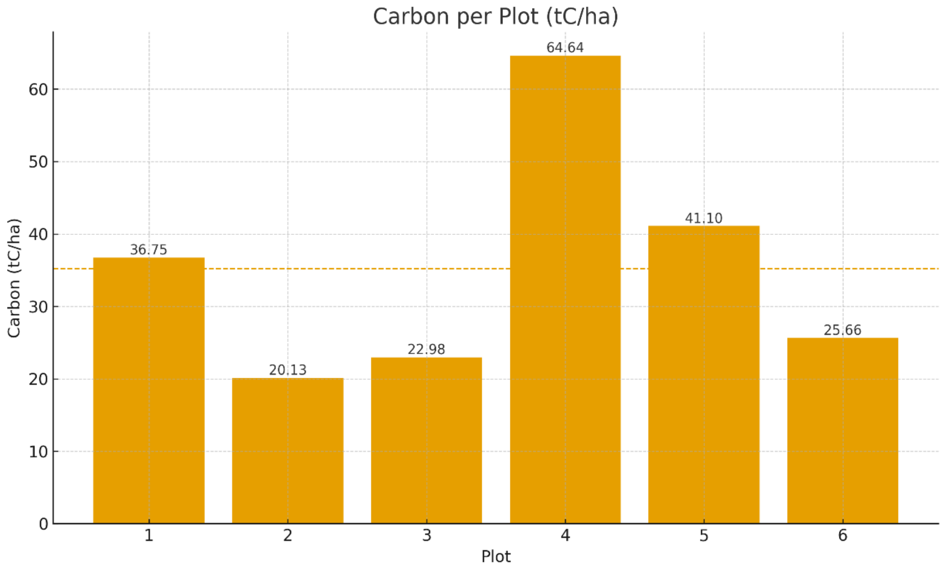

Figure 2. Carbon stock by plot (tC ha^{-1})

These patterns are consistent with ecological principles governing carbon storage, where stands with larger trees and denser canopies tend to accumulate more carbon. Lower values may reflect open canopy conditions, recent disturbance such as harvesting or fire, or differences in species composition. From a management perspective, this variation provides useful guidance for conservation planning. High-carbon stands should be prioritized for protection and monitoring, whereas lower-carbon areas may benefit from targeted restoration to enhance canopy development and carbon accumulation. The observed variability also highlights the importance of considering stand-level differences when scaling carbon estimates to larger landscape areas.

Results of Satellite Image Analysis

Sentinel-2 imagery acquired on 1 December 2024 was processed to derive three vegetation indices—NDVI, SAVI, and MSAVI2—which were then converted into fractional green vegetation cover (FC) maps before pixel-based estimation of aboveground carbon (Figure 3a–3c). The FC derived from NDVI (FC_NDVI) produced carbon densities ranging from 0.0094 to 0.6927 tC per pixel, corresponding to a total carbon stock of approximately 1,464.81 tC across the study area. The FC_SAVI results showed slightly higher pixel values (0.0186–0.7920 tC per pixel) and a similar total carbon stock of about 1,465.08 tC. In contrast, FC_MSAVI2 exhibited the largest range (0.1100–1.0653 tC per pixel) and generated the highest total carbon estimate, reaching 1,752.91 tC. These differences likely reflect the varying sensitivity of the vegetation indices to canopy density and soil background effects within the heterogeneous forest landscape.

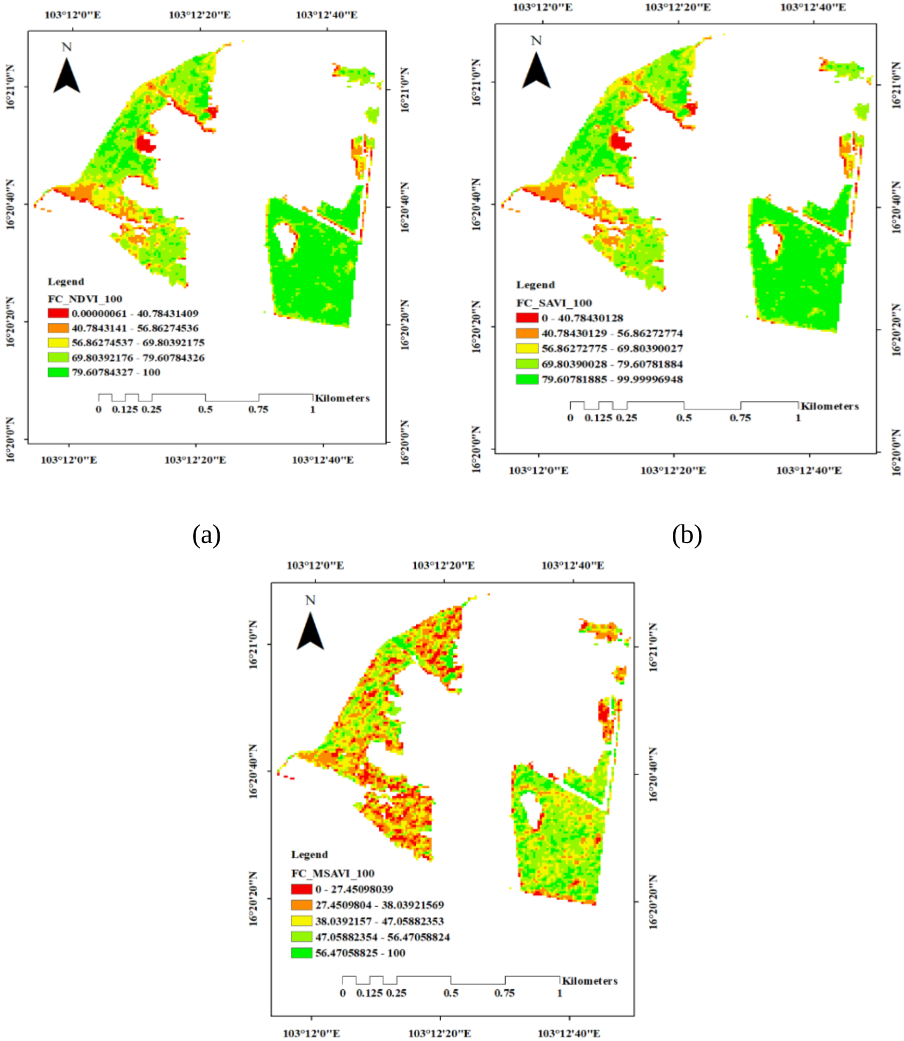

(a) (b)

(c)

Figure 3. Results of Satellite Image Analysis (a) FC_NDVI, (b) FC_SAVI, and (c) FC_MSAVI2

Spatially, the FC maps clearly distinguished variations in canopy density that were consistent with field observations. In the FC_NDVI and FC_SAVI layers, red to orange tones (0–56.862) represent unvegetated or impervious surfaces such as roads and bare soil, whereas yellow to light green (56.862–79.607) corresponds to moderately vegetated areas, including grasses and open shrublands. Dark green shades (79.607–100) indicate dense vegetation characterized by overlapping tree crowns.

For the FC_MSAVI2 map, the classification thresholds were adjusted to 0–38.039, 38.039–56.470, and 56.470–100 to improve the separation between bare soil and sparsely vegetated pixels. Among the three indices, FC_MSAVI2 produced the highest maximum pixel values and total carbon estimates. This result is consistent with the design of MSAVI2, which reduces soil background effects and minimizes saturation in areas with low leaf area index (LAI).

In contrast, the relatively lower values observed in FC_NDVI and FC_SAVI may be related to the early dry-season image acquisition, when canopy greenness and leaf water content were reduced. These conditions can decrease vegetation index responses and may lead to partial underestimation of biomass. Additional differences may arise from the spatial scale mismatch between Sentinel-2 pixels (10 m) and field plots (40×40 m), as well as possible co-registration errors and mixed-pixel effects within heterogeneous canopies. This study used a single-date Sentinel-2 image, which may also affect the results. Vegetation condition can change over time, especially in dry forests. Leaf cover and moisture vary between seasons, which can influence vegetation index values and may cause underestimation or overestimation of biomass.

In future work, multi-temporal data should be used. Images from different seasons can improve model accuracy. This approach can better capture seasonal changes and provide more reliable biomass and carbon estimation. Overall, the analysis demonstrates that Sentinel-2–derived FC maps effectively represent spatial variation in canopy density. Vegetation indices that better account for soil background influence, such as MSAVI2, tend to provide more reliable carbon estimates for mixed forest landscapes in northeastern Thailand.

Exponential Regression Model Analysis

This section analyzes the relationship between Fractional Vegetation Cover (FC) derived from Sentinel-2 imagery and Aboveground Biomass (AGB) using an exponential regression model (Figure 4; Table 3). The three vegetation indices—NDVI, SAVI, and MSAVI2—were compared to evaluate their ability to estimate carbon storage across the forest area.

NDVI produced carbon storage values ranging from 0.0094 to 0.6927 tC per pixel, with a total of 1,464.808 tC, while SAVI ranged between 0.0186 and 0.7920 tC per pixel, giving a total of 1,465.034 tC. In contrast, MSAVI2 yielded the widest range (0.1100–1.0653 tC per pixel) and the highest total carbon storage of 1,752.866 tC. When compared with field-based measurements (1,807.721 tC), all indices slightly underestimated total carbon; however,

MSAVI2 provided estimates most consistent with observed values.

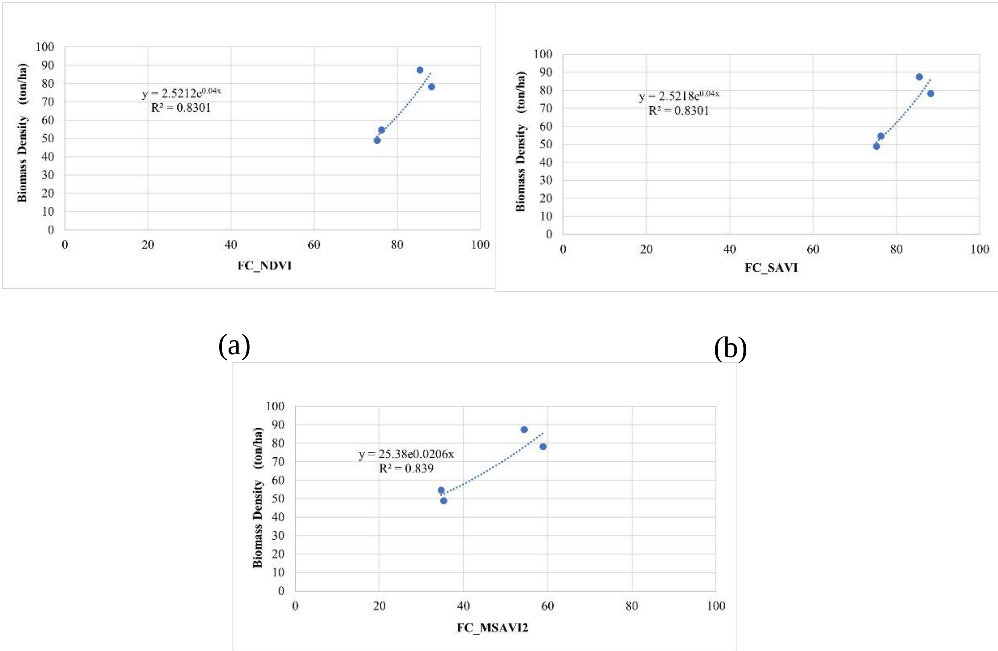

(a) (b)

(c)

Figure 4. Relationship Between Fractional Cover and Aboveground Biomass (a) NDVI, (b) SAVI, and (c) MSAVI2

Table 3. Comparison of Carbon Storage Estimated by Vegetation Indices and Field Data

Index	NDVI (tC)	SAVI (tC)	MSAVI2 (tC)	Field Data (tC)
Carbon Storage	1,464.808	1,465.034	1,752.866	1,807.721

The comparative results demonstrate that all indices can effectively estimate aboveground carbon storage, but MSAVI2 exhibited the strongest performance, attributed to its ability to minimize soil-background noise and capture canopy structure more accurately than NDVI or SAVI. Statistical validation further confirmed this trend, as MSAVI2 achieved the highest coefficient of determination (R^2=0.839) and formed the best exponential relationship with AGB, described by Equation 9.

$$AGB = 25.38 \times e^{(0.0206\ FC)}\ (R^2 = 0.839) \qquad (8)$$

where AGB represents the estimated aboveground biomass (kg per plot), and FC denotes the fractional vegetation cover (%) derived from MSAVI2.

Collectively, these findings confirm that MSAVI2 is a reliable and accurate approach for estimating forest biomass and carbon stocks. Its sensitivity to canopy greenness and density makes it suitable for mapping forest carbon dynamics in northeastern Thailand. The results also highlight its potential use in sustainable forest management, carbon accounting, and carbon-credit verification.

The exponential relationship between fractional vegetation cover and aboveground biomass reflects the typical growth pattern of tropical forests. Carbon accumulates rapidly during early stages and then stabilizes as the canopy matures. This nonlinear pattern agrees with Laosuwan *et al.,* (2025c), who reported that biomass and carbon accumulation often follow asymptotic trends controlled by physiological and structural limitations.

MSAVI2 performed better than NDVI and SAVI because it reduces soil background effects and detects intermediate canopy density more effectively. This advantage is important in dry deciduous and mixed forests, where seasonal leaf loss and heterogeneous canopy structure often cause underestimation when using traditional indices.

The close agreement between satellite-derived and field-measured carbon stocks (1,752.9 vs. 1,807.7 t C) supports the reliability of Sentinel-2 indices for regional biomass estimation. Integrating this exponential model into Thailand's T-VER and VCS carbon-credit frameworks could improve cost-effective monitoring, reporting, and verification (MRV) of forest carbon projects, while supporting sustainable forest management and climate-change mitigation.

Model Accuracy Assessment

The model accuracy assessment demonstrated the effectiveness of Sentinel-2–derived vegetation indices (VIs) for estimating aboveground biomass (AGB). When compared with field observations, all three indices (NDVI, SAVI, and MSAVI2) showed strong agreement, with absolute errors below 1.1 $t \cdot ha^{-1}$ and relative errors under 2%. These results indicate that Sentinel-2 VIs can provide reliable biomass estimates across heterogeneous forest conditions.

Among the evaluated indices, SAVI produced the highest accuracy, with the lowest RMSE (0.901 $t \cdot ha^{-1}$) and RMSE% (1.34%). This suggests that SAVI can reduce soil background effects, especially in areas with moderate canopy cover. MSAVI2 showed slightly higher error values (RMSE=1.013 $t \cdot ha^{-1}$; RMSE%=1.51%) but achieved the strongest correlation with field data (R^2=0.839). This indicates that MSAVI2 better represents vegetation structure. NDVI also showed a clear relationship with biomass, but its error was higher (RMSE=1.042 $t \cdot ha^{-1}$; RMSE%=1.55%), and it tended to underestimate carbon stocks. This may be related to canopy complexity and mixed-pixel effects.

The comparison among indices shows that the choice of index depends on the objective. SAVI is suitable when the goal is to reduce prediction error. MSAVI2 is more suitable when the goal is to represent canopy variation and structure. NDVI can still be used as a reference, but it should be applied with caution in complex forest conditions. These results also support the use of

Sentinel-2 data for carbon monitoring. The low error values indicate that this approach can be used as a cost-effective tool for carbon assessment and verification.

The observed variation in biomass and carbon stock reflects differences in forest structure across the study area. Plots with higher values are likely related to larger trees and denser canopy cover, which supports greater carbon accumulation. In contrast, lower values may indicate open canopy, younger stands, or past disturbance. This shows that forest structure strongly influences carbon storage. In dry dipterocarp forests, seasonal leaf loss and uneven canopy cover can limit biomass accumulation and affect vegetation index response. These findings suggest that areas with high carbon density should be prioritized for conservation, while areas with low carbon density may be improved through restoration. This approach can support both forest management and climate change mitigation.

CONCLUSIONS

This study demonstrated that an exponential regression model can effectively estimate aboveground biomass (AGB) and carbon stocks using Sentinel-2–derived vegetation indices. Field measurements collected from representative plots were successfully integrated with remotely sensed indices (NDVI, SAVI, and MSAVI2) to evaluate model performance and estimation accuracy. All three indices produced low prediction errors (RMSE<1.1 $t{\cdot}ha^{-1}$; RMSE% < 2%), indicating that satellite-based approaches can reliably quantify forest carbon stocks across heterogeneous environments.

Among the evaluated indices, MSAVI2 showed the highest explanatory power (R^2=0.839) and the smallest difference between field-measured and estimated carbon stocks (1752.87 vs. 1807.72 t C). This result suggests that MSAVI2 is more effective in reducing soil background influence and capturing variations in vegetation density and canopy structure. SAVI, however, produced the lowest RMSE and RMSE%, indicating the highest predictive accuracy among the tested models. Therefore, SAVI may be preferable when minimizing estimation error is the primary objective. NDVI retained its usefulness as a reference index but showed comparatively higher errors and a tendency to underestimate carbon stocks, likely due to its sensitivity to canopy structural complexity and mixed-pixel effects.

The integration of field inventory data with remote sensing indices proved to be a practical approach for estimating biomass and carbon stocks in forest ecosystems. The findings provide methodological guidance for selecting vegetation indices according to study objectives: MSAVI2 may be more suitable for explanatory modeling and optimization-based predictions, SAVI for reducing estimation error, and NDVI for benchmarking purposes. Importantly, the results highlight the potential of Sentinel-2 imagery as a cost-effective and scalable tool for national greenhouse gas inventories and carbon-credit initiatives, including Thailand’s T-VER and the Verified Carbon Standard (VCS).

Future research should focus on incorporating advanced analytical approaches, such as machine learning algorithms and multi-temporal analysis, as well as integrating higher-resolution validation data from UAV or LiDAR systems. These improvements could enhance prediction accuracy and expand the applicability of remote sensing–based biomass models across diverse forest conditions. Overall, remote sensing approaches have strong potential to support climate change mitigation, sustainable forest management, and the continued development of carbon-credit markets.

ACKNOWLEDGEMENTS

This research project is financially supported by Mahasarakham University.

CONFLICT OF INTEREST STATEMENT

The authors declare no conflict of interest.

REFERENCES

Andreoni, V., & Galmarini, S. (2016). Drivers in CO_2 emissions variation: A decomposition analysis for 33 world countries. Energy, 103, 27–37. https://doi.org/10.1016/j.energy.2016.02.145

Aneseyee, A. B., Soromessa, T., Elias, E., & Feyisa, G. L. (2021). Allometric equations for selected *Acacia* species (*Vachellia* and *Senegalia genera*) of Ethiopia. Carbon Balance and Management, 16, 34. https://doi.org/10.1186/s13021-021-00187-w

Angkahad, T., Chokkuea, W., Sangpradid, S., Uttaruk, Y., Viriyasatr, K., & Laosuwan, T. (2025). The assessment of aboveground biomass and carbon sequestration in community forests using UAV technology. Defense Technology Academy Journal, 7(15), R11–R28.

Angkahad, T., Laosuwan, T., Sangpradid, S., Prasertsri, N., Uttaruk, Y., Phoophathong, T., & Nuchthapho, J. (2024). An empirical analysis of aboveground biomass and carbon sequestration utilizing UAV photogrammetry and machine learning techniques. IEEE Access, 12, 186740–186752. https://doi.org/10.1109/ACCESS.2024.3514074

Askar, N., Nuthammachot, N., Phairuang, W., Wicaksono, P., & Sayektiningsih, T. (2018). Estimating aboveground biomass on private forest using Sentinel-2 imagery. Journal of Sensors, 2018, 1–11. https://doi.org/10.1155/2018/6745629

Awichin, P., Laosuwan, T., Sangpradid, S., Uttaruk, Y., Phoophathong, T., Leammanee, S., & Nuchthapho, J. (2025). UAV multispectral indices and linear regression for estimating biomass and carbon in rubber plantations. IEEE Access, 13, 215845. https://doi.org/10.1109/ACCESS.2025.3644408

Bullock, E. L., & Woodcock, C. E. (2021). Carbon loss and removal due to forest disturbance and regeneration in the Amazon. Science of the Total Environment, 764, 142839. https://doi.org/10.1016/j.scitotenv.2020.142839

Carpio, A., Ponce-Lopez, R., & Lozano-García, D. F. (2021). Urban form, land use, and cover change and their impact on carbon emissions in the Monterrey metropolitan area, Mexico. Urban Climate, 39, 100947. https://doi.org/10.1016/j.uclim.2021.100947

Duangsathaporn, K., Sangram, N., Omule, Y., Prasomsin, P., Palakit, K., & Lumyai, P. (2023). Formulating equations for estimating forest stand carbon stock for various tree species groups in northern Thailand. Forests, 14(8), 1584. https://doi.org/10.3390/f14081584

Faria, L. D. D., Matricardi, E. A. T., Marimon, B. S., Miguel, E. P., Junior, B. H. M., Oliveira, E. A. D., Prestes, N. C. C. D. S., & Carvalho, O. L. F. D. (2024). Biomass prediction using Sentinel-2 imagery and an artificial neural network in the Amazon/Cerrado transition region. Forests, 15(9), 1599. https://doi.org/10.3390/f15091599

Grantham Research Institute on Climate Change and the Environment. (2023). What is the role of deforestation in climate change and how can reducing emissions from deforestation and degradation (REDD+) help? London School of Economics and Political Science. https://www.lse.ac.uk/granthaminstitute/explainers/whats-redd-and-will-it-help-tackle-climate-change/

Houghton, R. A., Hall, F., & Goetz, S. J. (2009). Importance of biomass in the global carbon cycle. Journal of Geophysical Research: Biogeosciences, 114(G2), G00E03. https://doi.org/10.1029/2009JG000935

Huete, A. R. (1988). A soil-adjusted vegetation index (SAVI). Remote Sensing of Environment, 25(3), 295–309. https://doi.org/10.1016/0034-4257(88)90106-X

Intergovernmental Panel on Climate Change (IPCC). (2006). 2006 IPCC guidelines for national greenhouse gas inventories. Institute for Global Environmental Strategies (IGES).

Intergovernmental Panel on Climate Change (IPCC). (2014). Climate change 2014: Synthesis report. IPCC.

Israel, R., Akintunde-Alo, D. A., & Oluwajuwon, T. V. (2025). Comparative evaluation of Landsat 9 vegetation indices for estimating urban forest biomass in the botanical garden of the University of Ibadan, Nigeria. Discover Forestry, 1, 32. https://doi.org/10.1007/s44415-025-00031-2

Kulawardhana, R. W., Popescu, S. C., & Feagin, R. A. (2014). Fusion of LiDAR and multispectral data to quantify salt marsh carbon stocks. Remote Sensing of Environment, 154, 345–357. https://doi.org/10.1016/j.rse.2014.08.018

Kulmann, M. S. de S., Eufrade-Junior, H. de J., Dick, G., Schumacher, M. V., Azevedo, G. B. de, Azevedo, G. T. de O. S., & Guerra, S. P. S. (2022). Belowground biomass harvest influences biomass production, stock, export and nutrient use efficiency of second rotation Eucalyptus plantations. Biomass and Bioenergy, 161, 106476. https://doi.org/10.1016/j.biombioe.2022.106476

Laosuwan, T., Itsarawisut, J., Uttaruk, Y., Sangpradid, S., Rotjanakusol, T., & Peebkhunthod, T. (2025b). Urban tree carbon stock assessment based on remote sensing and field inventory data. Agriculture and Forestry, 71(4), 17–35. https://doi.org/10.17707/AgricultForest.71.4.02

Laosuwan, T., Rotjanakusol, T., Chokkuea, W., Singharath, M., & Itsarawisut, J. (2025a). Creation of technique for assessing aboveground biomass and carbon sequestration using unmanned aerial vehicles. Geographia Technica, 20(2), 65–78. https://doi.org/10.21163/GT_2025.202.06

Laosuwan, T., Uttaruk, Y., Nakapan, S., Itsarawisut, J., & Plybour, C. (2025c). Evaluation of tree biomass and carbon sequestration through remote sensing and field methods. Geographia Technica, 20, 33–43. https://doi.org/10.21163/GT_2025.201.04

Laosuwan, T., Uttaruk, Y., Sangpradid, S., Butthep, C., & Leammanee, S. (2023). The carbon sequestration potential of silky oak (*Grevillea robusta*). Forests, 14(9), 1824. https://doi.org/10.3390/f14091824

Liu, P., Ren, C., Yang, X., et al. (2024). Combining Sentinel-2 and diverse environmental data largely improved aboveground biomass estimation in China's boreal forests. Scientific Reports, 14, 27528. https://doi.org/10.1038/s41598-024-27528

McNicol, I. M., Ryan, C. M., & Mitchard, E. T. A. (2018). Carbon losses from deforestation and widespread degradation offset by extensive growth in African woodlands. Nature Communications, 9, 3045. https://doi.org/10.1038/s41467-018-05386-z

Mkuzi, H. T., Ocansey, C. M., Maghanga, J., Gulyás, M., Penksza, K., Szentes, S., Michéli, E., Fuchs, M., & Boros, N. (2025). A review of biomass estimation methods for forest ecosystems in Kenya. Land, 14(9), 1873. https://doi.org/10.3390/land14091873

Mutanga, O., Adam, E., & Cho, M. A. (2012). High density biomass estimation for wetland vegetation using WorldView-2 imagery. International Journal of Applied Earth Observation and Geoinformation, 18, 399–406. https://doi.org/10.1016/j.jag.2012.03.012

Ogawa, H., Yoda, K., Ogino, K., & Kira, T. (1965). Comparative ecological studies on three main types of forest vegetation in Thailand II: Plant biomass. Nature and Life in Southeast Asia, 4, 49–80.

Pearson, T. R. H., Brown, S., Murray, L., & Sidman, G. (2017). Greenhouse gas emissions from tropical forest degradation: An underestimated source. Carbon Balance and Management, 12(1), 3. https://doi.org/10.1186/s13021-017-0072-2

Plybour, C., Laosuwan, T., Uttaruk, Y., Awichin, P., Rotjanakusol, T., Itsarawisut, J., & Singharath, M. (2025). Plant species diversity, above-ground biomass, and carbon stock in a dry dipterocarp forest. Diversity, 17(6), 428. https://doi.org/10.3390/d17060428

Qi, J., Chehbouni, A., Huete, A. R., Kerr, Y. H., & Sorooshian, S. (1994). A modified soil-adjusted vegetation index (MSAVI2). Remote Sensing of Environment, 48(2), 119–126. https://doi.org/10.1016/0034-4257(94)90134-1

Ritchie, H. (2021). Deforestation and forest loss. Our World in Data. https://ourworldindata.org/deforestation

Samek, J., Skole, D. L., Klinhom, U., Laosuwan, T., Uttaruk, P., & Butthep, C. (2014). Smallholders in Thailand and REDD+ and FLEGT linkages. Tropenbos International.

Samphutthanont, R., Suppawimut, W., Kitthitinan, P., & Promsopha, K. (2024). Carbon sequestration assessment using satellite data and GIS. Environment and Natural Resources Journal, 22(6), 574–584. https://doi.org/10.32526/ennrj/22/20240183

Somprasong, K. (2024). Estimation of potential carbon sequestration in Thai reforestation from mining. Carbon Management, 15(1). https://doi.org/10.1080/17583004.2024.2347883

Sousa Júnior, V. D. P., Sparacino, J., Espindola, G. M. D., & Assis, R. J. S. D. (2023). Carbon biomass estimation using vegetation indices in agriculture–pasture mosaics. ISPRS International Journal of Geo-Information, 12(9), 354. https://doi.org/10.3390/ijgi12090354

Sun, X., Wang, Q., & Song, G. (2024). Revisiting generic allometric equations for estimating forest aboveground biomass in Japan. Biomass and Bioenergy, 180, 107025. https://doi.org/10.1016/j.biombioe.2023.107025

Thailand Greenhouse Gas Management Organization (TGO). (2017). Plot design and data collection for forestry projects. https://ghgreduction.tgo.or.th/th/download-tver/68-tver-publications/349-2017-11-28-07-52-18.html

Tucker, C. J. (1979). Red and photographic infrared linear combinations for monitoring vegetation. Remote Sensing of Environment, 8, 127–150. https://doi.org/10.1016/0034-4257(79)90013-0

United Nations Framework Convention on Climate Change (UNFCCC). (1992). United Nations Framework Convention on Climate Change. United Nations.

United Nations Framework Convention on Climate Change (UNFCCC). (2010). Report of the Conference of the Parties on its fifteenth session. UNFCCC.

Uttaruk, Y., & Laosuwan, T. (2018). Community forest for global warming mitigation: The technique for estimation of biomass and aboveground carbon storage using remote sensing method. Agriculture and Forestry, 64(3), 47–57. https://doi.org/10.17707/AgricultForest.64.3.04

Uttaruk, Y., & Laosuwan, T. (2020a). Comparison of carbon storage measurement methods on agroforestry systems in Sakon Nakhon Province. Scientific Journal of King Faisal University, 21(2), 95–99.

Uttaruk, Y., & Laosuwan, T. (2020b). Methods of estimation for aboveground carbon stock in Nongbua-Nonmee community forest. Agriculture and Forestry, 66(3), 183–195.

Uttaruk, Y., Laosuwan, T., Sangpradid, S., Butthep, C., Rotjanakusol, T., Sittiwong, W., & Nilrit, S. (2024). Thailand's urban forestry programs assisted by ecological and economic valuation. Land, 13(9), 1440. https://doi.org/10.3390/land13091440

Uttaruk, Y., Laosuwan, T., Sangpradid, S., Samek, J. H., Butthep, C., Rotjanakusol, T., Dumrongsukit, S., & Rouylarp, Y. (2026). Species-specific allometric models for biomass and carbon stock estimation in silver oak plantation forests. Forests, 17(1), 100. https://doi.org/10.3390/f17010100

Vahtmäe, E., Kotta, J., Lõugas, L., & Kutser, T. (2021). Mapping spatial distribution and biomass of benthic vegetation using hyperspectral and Sentinel-2 sensors. International Journal of Applied Earth Observation and Geoinformation, 102, 102444. https://doi.org/10.1016/j.jag.2021.102444

Vicharnakorn, P., Shrestha, R. P., Nagai, M., Salam, A. P., & Kiratiprayoon, S. (2014). Carbon stock assessment using remote sensing and forest inventory data in Lao PDR. Remote Sensing, 6(6), 5452–5479. https://doi.org/10.3390/rs6065452

Yu, L., Fan, L., Ciais, P., Xiao, J., Frappart, F., Sitch, S., Chen, J., Xiao, X., Fensholt, R., Chang, Z., Fang, H., Li, X., Cui, T., Ma, M., & Wigneron, J.-P. (2024). Forest degradation contributes more to carbon loss than forest cover loss. International Journal of Applied Earth Observation and Geoinformation, 128, 103729. https://doi.org/10.1016/j.jag.2024.103729